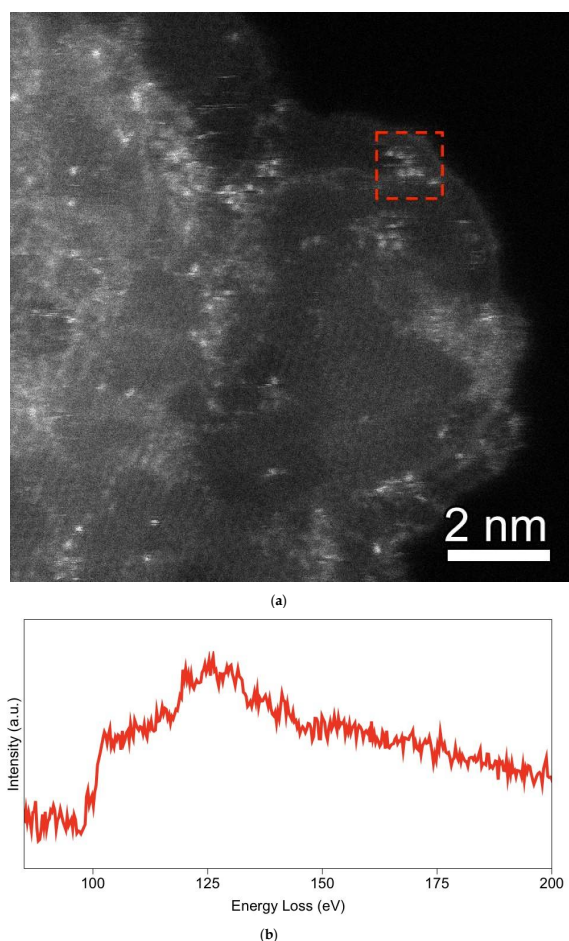


# Supplementary Materials: An Atomistic Carbide-Derived Carbon Model Generated Using ReaxFF-Based Quenched Molecular Dynamics

Matthew W. Thompson , Boris Dyatkin , Hsiu-Wen Wang , C. Heath Turner, Xiahan Sang , Raymond R. Unocic , Christopher R. Iacovella , Yury Gogotsi , Adri C. T. van Duin  and Peter T. Cummings 

## 1. Electron Energy Loss Spectroscopy

Aberration Corrected Scanning Transmission Electron Microscopy (ADF-STEM) and Electron Energy Loss Spectroscopy (EELS) data were collected on CDC samples. Data collected on a SiC-CDC sample vacuum annealed at 700 °C is shown in Figure S1. A number of bright spots are observed and are further investigated with EELS. An EEL spectra was collected on the region highlighted in a red box and a K-edge at 99 eV was observed. This corresponds to Si, indicating that bright spots in the sample are residual Si atoms not fully processed during material synthesis.



**Figure S1.** Annular Dark-Field (ADF) Aberration-Corrected Scanning Transmission Electron Microscopy (STEM) image and Electron Energy Loss (EEL) spectra collected on a SiC-CDC sample after vacuum annealing at 700 °C. (a) ADF STEM image of SiC-CDC vacuum annealed at 700 °C; (b) Corresponding EEL spectra from SiC-CDC vacuum annealed at 700 °C. The K-edge at 99 eV confirms that the bright spots located in the region highlighted with a red box are Si atoms.

## 2. Raman Spectroscopy

A Raman spectrum is included in Figure S2. The data is characteristic of disordered carbon and shows prominent D and G bands.

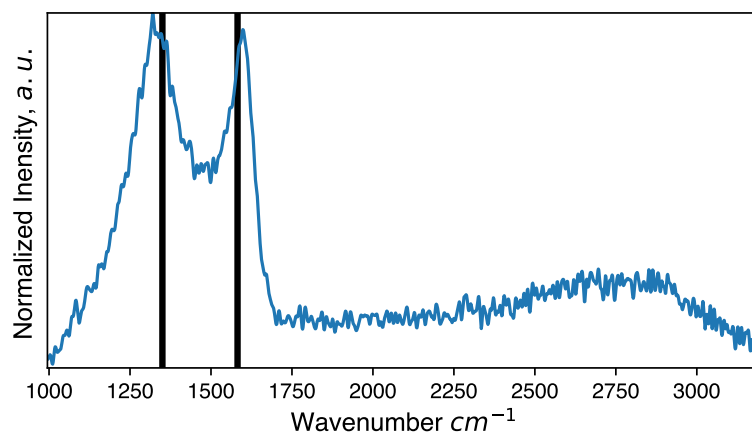


Figure S2. Raman spectrum of experimental sample.

## 3. Effects of Compression Pressure

The compression procedure described in the main text was repeated at pressures 1000 atm, 10,000 atm, 30,000 atm, 50,000 atm in addition to the selected pressure of 20,000 atm. System densities over the course of these compressions are shown in Figure S3. It is observed that pressures of 1000 atm and 10,000 atm are too low to largely impact the density. A barostat of 50,000 atm is too large, as it compresses the system nearly to the graphitic limit of  $2.26 \text{ g cm}^{-3}$ . Intermediate pressures of 20,000 atm and 30,000 atm increase the density of the system above the density observed in experiment but not so high that they could not be found in certain nanostructures found in CDCs.

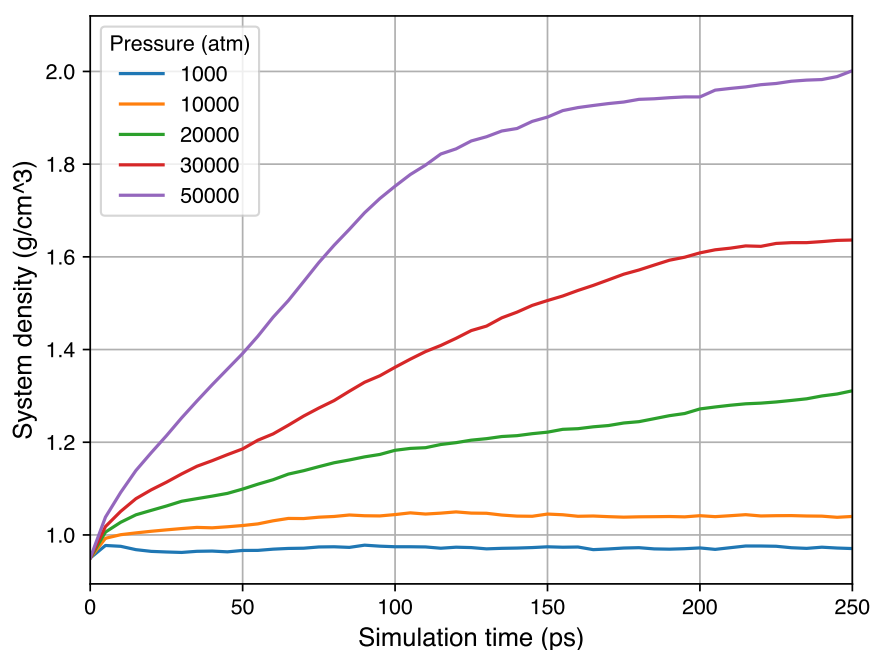
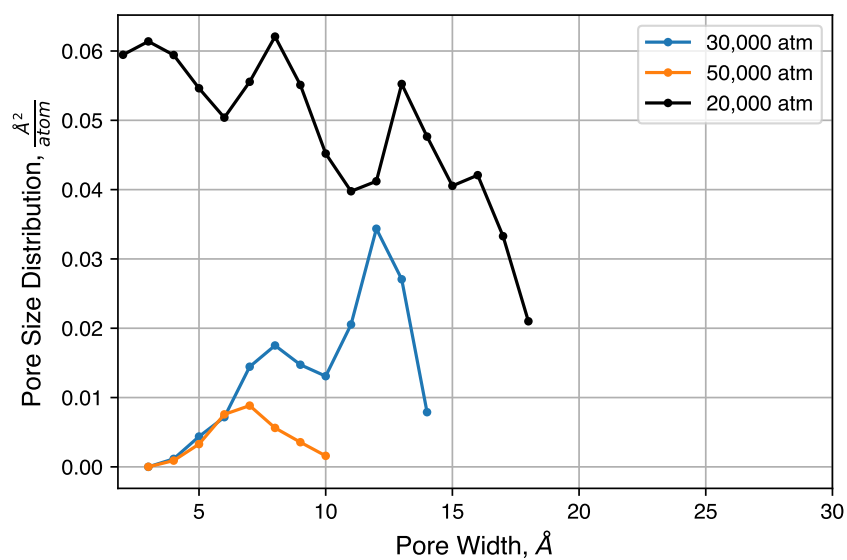


Figure S3. System densities over the length of compression simulations with different reference pressures.

Effects of compression pressure on pore size distribution are also explored, using methods described in the main text and shown in Figure S4. As implied in the densities of systems compressed above 20,000 atm, overall pore volume is greatly reduced in systems compressed at these pressures. Therefore, in order to minimize the loss of pore volume as a result of compression but benefit from the reduction in average pore size, a pressure of 20,000 atm was selected.



**Figure S4.** Pore size distributions resulting from the use of barostats with high reference pressure.